Cross-calibration of Polar-Orbiting Ocean-Color Sensors Using Geostationary Observations

R. Frouin[1], J. Tan[1], and H. Murakami[2]

[1]*Scripps Institution of Oceanography, University of California San Diego, La Jolla, California, USA*

[2]*Earth Observation Research Center, Japanese Aerospace Exploration Agency, Tsukuba, Japan*

Introduction

-Radiometric cross-calibration of optical (e.g., ocean-color) instruments is an important activity to ensure product consistency and generate climate data records.

-It can be easily defined as viewing the same radiance at the same time, but it is much more difficult to achieve during in flight operations of different sensors on different orbits.

-Apart from viewing the Moon, one must rely on measuring the solar radiation reflected by the Earth-atmosphere system at the same time and location because of its time variability.

-The Earth-atmosphere system has generally some bidirectional reflectance function that requires observing under the same solar and viewing geometry (i.e., same line of sight).

-If the spectral bands to be compared do not have the same or close definition, some empirical transformation must be applied to make the comparison thus the cross-calibration.

Methodology

-The methodology examined utilizes a sensor onboard a satellite in geostationary orbit, which acts as an intermediary between the polar-orbiting sensors to calibrate (e.g., MODIS-A and MODIS-T).

-Compared with other cross-calibration techniques (Moon, desert sites), the advantage is that precise coincidences in time and geometry are easier to find (i.e., more numerous).

-Many coincidences occur over oceanic regions, allowing the cross-calibration to be performed at radiance levels typically encountered in ocean-color remote sensing.

-It may not be possible to cross-calibrate the polar-orbiting sensors in all their spectral bands. Only those bands closest to the spectral bands of the GEO sensor, or the combinations of bands that correlate satisfactorily with its spectral bands, are selected.

-Consider the cross-calibration of two polar-orbiting sensors and assume for simplicity that polar-orbiting and geostationary sensors observe at the same time (t or t'). The cross-calibration coefficients between each polar-orbiting sensor and the geostationary sensor, A_{1i} and A_{2j}, can be written:

$$A_{1i} = \rho_{ref}(t) / f_{1i}[\rho_{1i}(t)]$$

$$A_{2j} = \rho_{ref}(t') / f_{2j}[\rho_{2j}(t')]$$

where f_{1i} and f_{2j} are empirical functions that relate ρ_{1i} and ρ_{2j} to ρ_{ref}. These functions are determined theoretically, from simulations for realistic environment and geometry conditions.

-If the two sensors are perfectly inter-calibrated, A_{1i} is equal to A_{2j}. Differences between A_{1i} and A_{2j}, on the other hand, will indicate that the calibration of the two sensors is not consistent and, therefore, needs to be adjusted accordingly.

-Depending on the spectral band, the ρ_{ref} measurements may not be well correlated to ρ_1 and ρ_2 measurements in a single spectral band, but to measurements in several spectral bands. The formalism remains the same, but we now have:

$$A_{1M} = \rho_{ref}(t) / f_{1M}[\rho_{1i}(t), i = 1, 2, \ldots, M]$$

$$A_{2N} = \rho_{ref}(t') / f_{2N}[\rho_{2j}(t'), j = 1, 2, \ldots, N]$$

where the empirical functions f_{1M} et f_{2N} now relate ρ_{ref} to a combination of measurements ρ_{1i} in M spectral bands and ρ_{2j} in N spectral bands.

-Consequently, differences between A_{1M} and A_{2N} will only be indicative of calibration inconsistencies in combination of spectral bands, not single bands. If not complete, this information is useful, and A_{1M} should be equal to A_{2N} in any calibration normalization.

-The collocated pixels from the pairs of instruments to cross-calibrate, i.e., a low earth orbit (LEO) sensor and the geostationary (GEO) sensor of reference, must be observed under comparable conditions, which means close solar and viewing angles.

-The time difference between the LEO and GEO observations must also be sufficiently small to neglect changes in the reflectance characteristics of the atmosphere and target.

-Criteria to select suitable observations are based on the repeat cycle of the GEO sensor, the type of target, the radiometric noise, the accuracy of the spectral matching, and the impact on the measured reflectance.

-Since the LEO sensor has generally a strongly inclined (i.e., near polar) orbit, observations along the same line of sight by the LEO and GEO sensors are expected to occur near the equator, the only region where the viewing azimuth angles would match.

Application to cross-calibrating SGLI, MODIS-T, and -A

-AHI on Hiwamari-8 is the GEO sensor of reference.

-Cross-calibration is performed after system vicarious calibration.

***Table 1**: AHI and equivalent SGLI, MODIS-T, and MODIS-A spectral bands or combinations of spectral bands to cross-calibrate.*

AHI wavelength (nm)	SGLI wavelength (nm)	MODIS-A wavelength (nm)	MODIS-T wavelength (nm)
471	443&490	443&469, 443&488, 469&488, 469	443&469, 443&488, 469&488, 469
510	490&530	469&531, 469&547, 469&555, 488&531, 488&547, 488&555	469&531, 469&547, 469&555, 488&531, 488&547, 488&555
639	672	645, 667, 678	645, 667, 678
857	867	859, 869	859, 869
1610	1635	1640	1640
2257	2209	2130	2130

Cross-Calibration dates/times/locations

***Table 2**: The observation time, geometry, latitude/longitude, and total number of collocated pixels for each sensor pair on the three different dates considered.*

Sensor Pair	Date	No. of Pixels	Time (GMT)	Lat/Lon	Solar Zenith	View Zenith	Relative Azimuth	Scattering angle
AHI/ MODIS-T	11 May 2018	684	01:30 h	0.7°-2.0°N, 132.1°-132.7°E	26.9°-27.8°	8.7°-11.0°	44.3°-44.7°	157.7°-158.8°
	22 Jan 2019	257	01:30 h	0.5°-1.8°N, 132.3°-132.9°E	32.6°-33.4°	8.4°-10.7°	29.9°-34.6°	153.8°-155.4°
	25 Jan 2020	619	01:30 h	0.5°-2.0°N, 132.2°-132.8°E	32.5°-33.2°	8.5°-10.9°	28.6°-33.3°	154.1°-155.8°
AHI/ MODIS-A	11 May 2018	396	04:30 h	0°-1.5°S, 134.7°-135.3°E	30.1°-30.9°	5.6°-7.9°	128.0°-137.4°	143.9°-145.5°
	25 Jan 2020	381	04:30 h	0°-1.5°S, 134.7°-135.3°E	26.8°-27.4°	5.8°-7.9°	139.7°-149.1°	146.3°-148.0°
AHI/ SGLI	22 Jan 2019	418	01:50 h	2.0°-2.8°N, 126.7°-127.1°E	35.3°-35.8°	15.7°-17.6°	30.8°-31.5°	156.8°-157.8°
	25 Jan 2020	225	01:10 h	0.3°-0.6°N, 137.8°-138.1°E	32.7°-33.0°	2.5°-4.4°	29.2°-29.5°	149.3°-150.8°

Example of spectral matching (AHI/MODIS-T)

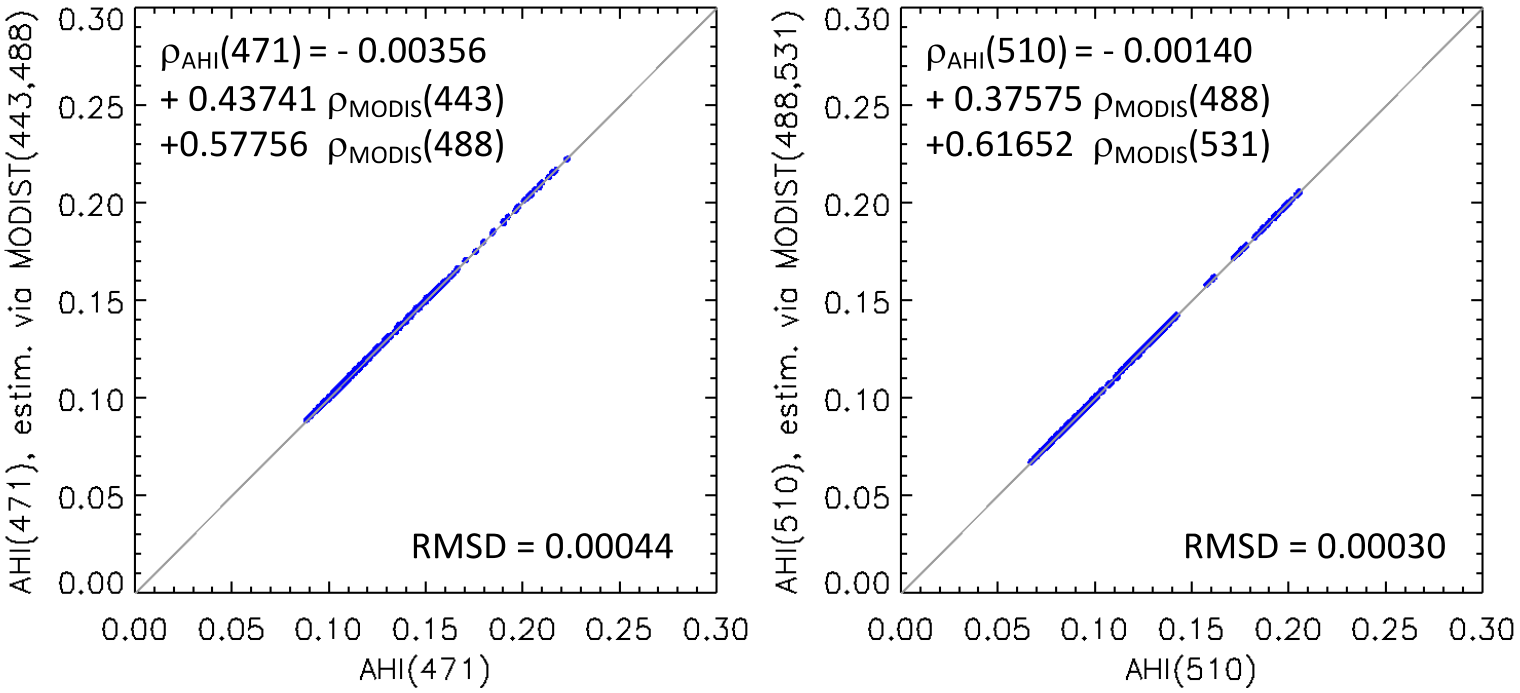

Figure 1: *Relation between the TOA reflectance in selected AHI and MODIS-T bands, i.e., MODIS-T at 443 and 488 nm vs. AHI at 471 nm (left), MODIS-T at 488 and 531 nm vs. AHI at 510 nm (right). Various geometries and geophysical conditions are used in 6SV simulations. Transformation of MODIS-T data at 667 nm into equivalent AHI data at 639 nm is less accurate due to gas absorption. In practice, relations obtained without gas absorption are used, and TOA signal is corrected for gas absorption.*

Example of remapped imagery (25 January 2020)

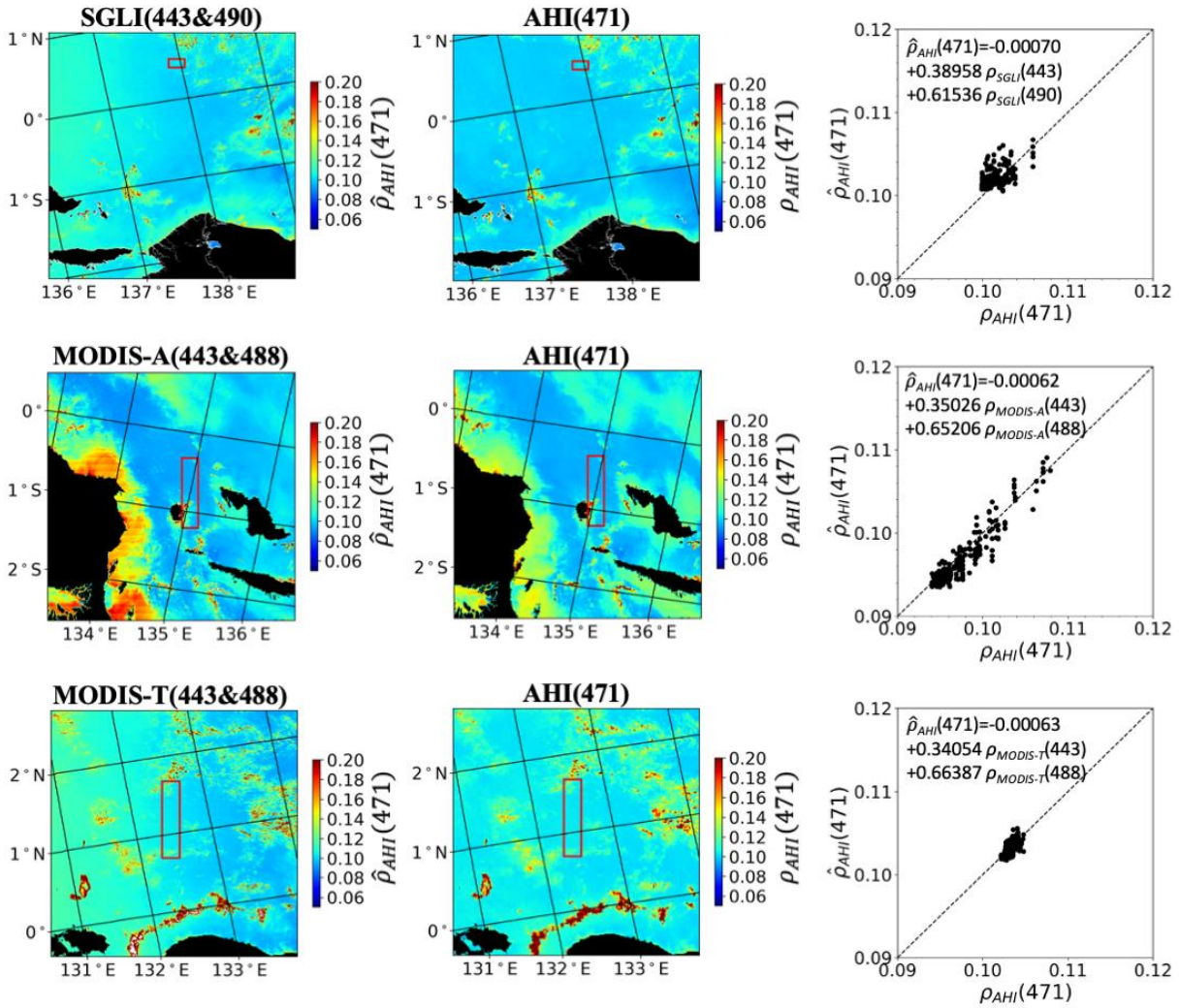

Figure 2: *Concomitant SGLI/AHI (01:10 GMT, top row), MODIS-A/AHI (04:30 GMT, middle row), and MODIS-T/AHI (01:30 GMT, bottom row) imagery acquired on 25 January 2020. Red rectangles indicate where the coincident pixels occur. The right panels show the scatter plots of equivalent versus measured AHI reflectance.*

Example of coincidences (25 January 2020)

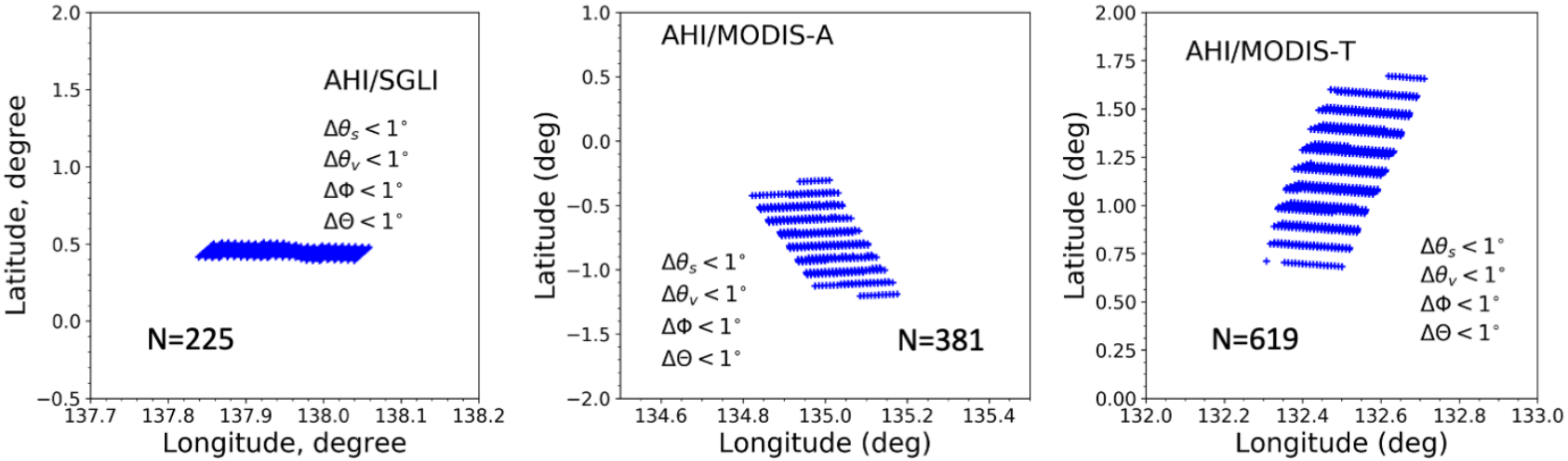

Figure 3: *Location of clear sky AHI/SGLI (01:10 GMT, 225 pixels in total, left), AHI/MODIS-A (04:30 GMT, 381 pixels in total, middle), and AHI/MODIS-T (01:30 GMT, 619 pixels in total, right) coincidences for 25 January 2020, i.e., differences in solar zenith ($\Delta\theta_s$), view zenith ($\Delta\theta_v$), relative azimuth ($\Delta\phi$), and scattering angle ($\Delta\Theta$) are less than 1°.*

Example of cross-calibration coefficients (AHI/MODIS-A)

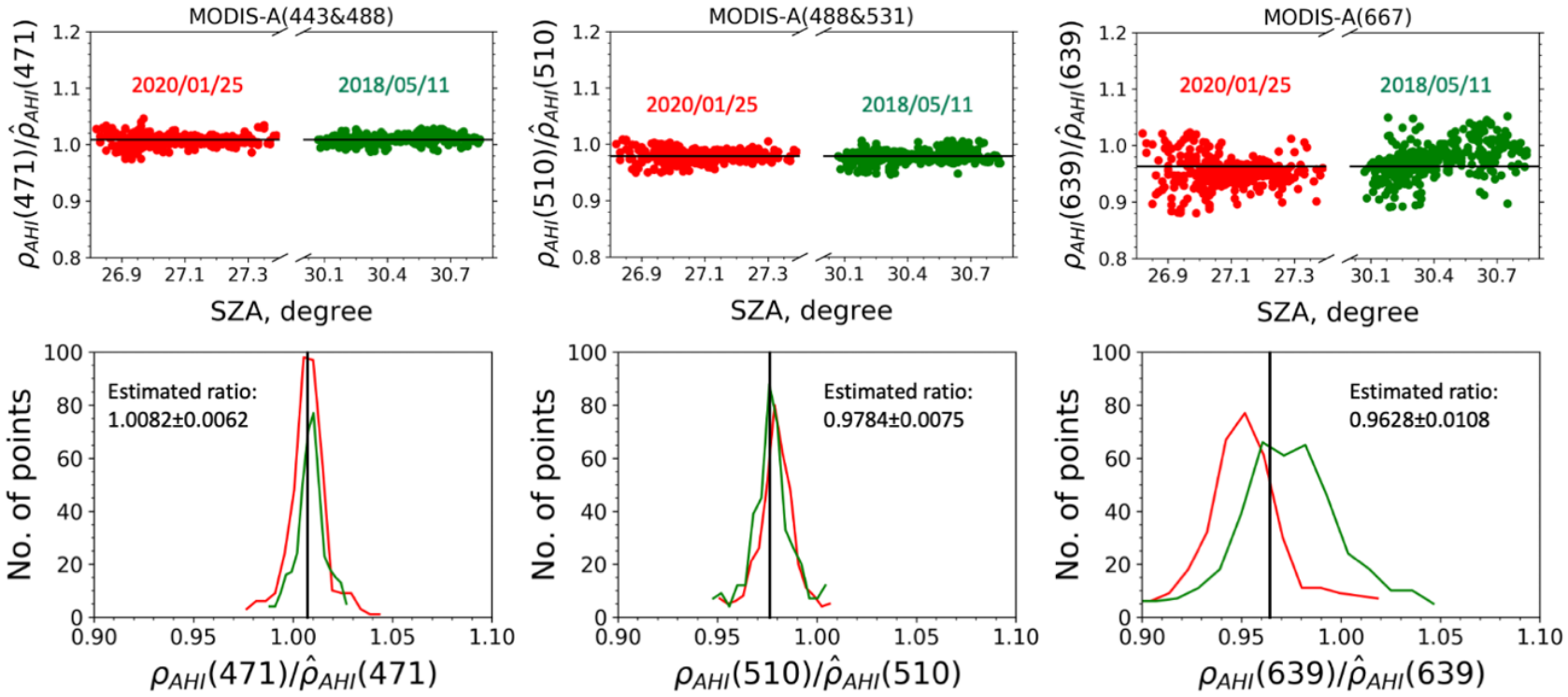

Figure 4: *(Top) cross-calibration coefficients versus SZA and (bottom) histograms of cross-calibration coefficients for AHI/MODIS-A at 471, 510, and 639 nm. The equivalent AHI reflectance $\hat{\rho}_{AHI}$ at 471, 510, and 569 nm were generated using MODIS-A 443&488 nm, 488&531 nm, and 667 nm, respectively. Different colors represent different dates, i.e., red – 2020/01/25, and green – 2018/05/11. Black lines (vertical and horizontal) indicate the estimated mean.*

Cross-calibration coefficients of LEO sensor pairs in polar orbit

***Table 3**. Cross-calibration coefficients A and associated uncertainties for SGLI/MODIS-A, SGLI/MODIS-T, and MODIS-A/MODIS-T, obtained using MODIS and SGLI band combinations.*

Sensor Pair	SGLI/MODIS-A	SGLI/MODIS-T	MODIS-A/MODIS-T
A(471) 469			0.9877±0.0075
A(471) 443&488/443&490	1.0192±0.0099	1.0166±0.0093	0.9974±0.0078
A(471) 443&469			0.9916±0.0075
A(471) 469&488			0.9942±0.0075
A(510) 488&531/490&530	1.0356±0.0136	1.0451±0.0125	1.0092±0.0094
A(510) 488&547			1.0096±0.0096
A(510) 488&555			1.0120±0.0109
A(510) 469&531			1.0065±0.0094
A(510) 469&547			1.0025±0.0096
A(510) 469&555			1.0056±0.0109
A(639) 645			1.0053±0.0161
A(639) 667/672	0.9664±0.0302	0.9796±0.0325	1.0136±0.0195
A(639) 678			1.0189±0.0214

Conclusions

-Using an intermediary sensor in GEO orbit allows one to find numerous coincident measurements in space, time, and geometry over oceanic regions (signal level for ocean-color applications), an advantage over other cross-calibration techniques.

-MODIS-A and MODIS-T after SVC are well cross-calibrated in the bands of reference, with differences of 1-2% from unity, generally within the uncertainties, for all band combinations.

-Using diverse band combinations further suggested that the MODIS-A and MODIS-T individual bands at 443, 469, 488, 531, 547, and 555 nm are also well cross-calibrated.

Conclusions (cont.1)

-In comparison, larger differences, i.e., 1.9%, 3.6%, and 3.3%, between SGLI and MODIS-A, were found for the equivalent AHI bands at 471, 510, and 639 nm. Similar results were obtained between SGLI and MODIS-T, with the differences of 1.7%, 4.5%, and 3.0%, respectively.

-These cross-calibration differences are above the estimated uncertainties except for SGLI/MODIS-T coefficients at 639 nm, affirming that significant differences exist between SGLI and MODIS-A and -T TOA signals, especially in the blue-green spectral range.

-This does not necessarily mean than water reflectance retrievals are less accurate with SGLI, because SVC was performed differently.

Conclusions (cont.2)

-One expects that the population variance will be closer to the actual one with an increased number of days, and the uncertainty reduced with an increased number of coincidences.

-Methodology is generic and generally applicable to optical sensors in polar orbit.

-Methodology has great potential in view of new GEO sensors, in particular GOCI-2, which has improved performance and ocean-color bands, allowing a more accurate and complete cross-calibration of ocean-color sensors in polar orbit.